



## Article

# Analysis of Aroma Volatiles from *Michelia crassipes* Flower and Its Changes in Different Flower Organs during Flowering

Yubing Yong <sup>1</sup>, Jieli Yuan <sup>1</sup>, Xiaoling Jin <sup>1,\*</sup>, Yu Huang <sup>2,\*</sup>, Zhe Zhang <sup>1</sup>, Yan Chen <sup>3</sup> and Minhuan Zhang <sup>1</sup>

<sup>1</sup> College of Landscape Architecture, Central South University of Forestry and Technology, Changsha 410004, China

<sup>2</sup> College of Art and Design, Nanning University, Nanning 530001, China

<sup>3</sup> School of Architecture and Art Design, Hunan University of Science and Technology, Changsha 411201, China

\* Correspondence: jxl0716@hotmail.com (X.J.); huangyu@nnxy.edu.cn (Y.H.)

**Abstract:** *Michelia crassipes* is a great ornamental plant, the flowers of which have high economic value. In this study, we employed headspace solid-phase microextraction (HS-SPME) combined with gas chromatography high-resolution mass spectrometry (GC-HRMS) for the first time to identify the volatile compounds emitted from different organs of *M. crassipes* flowers at different flowering stages. *M. crassipes* flower odor comprises 69 volatile compounds that are dominated by terpenes constituting 84% of collected volatiles. It was found that  $\alpha$ -guaiene,  $\beta$ -caryophyllene and germacrene B had the highest relative amounts, while ethyl 3-methyl valerate, methyl benzoate and  $\beta$ -damascone had the highest odor activity values (OAVs). This contributed to the complex fruity, woody and floral aromas of *M. crassipes*. Total odor emission increased along the flower blooming, which was most abundant in the pistil followed by tepals and stamens. Paraffin sections of *M. crassipes* flower organs showed the highest density of oil secretory cells in the pistil at the full flowering stage, which was positively correlated with total odor release. The scent of the pistil and tepals was characterized by terpenes, whereas stamens was characterized by benzenoids. We suggest that the benzenoids in stamens might contribute to pollinator attraction in *M. crassipes*.

**Keywords:** *Michelia L.*; floral scent compounds; flower organs; flowering stages; oil secretory cells



**Citation:** Yong, Y.; Yuan, J.; Jin, X.; Huang, Y.; Zhang, Z.; Chen, Y.; Zhang, M. Analysis of Aroma Volatiles from *Michelia crassipes* Flower and Its Changes in Different Flower Organs during Flowering. *Horticulturae* **2023**, *9*, 442. <https://doi.org/10.3390/horticulturae9040442>

Received: 15 February 2023

Revised: 26 March 2023

Accepted: 27 March 2023

Published: 28 March 2023



**Copyright:** © 2023 by the authors. Licensee MDPI, Basel, Switzerland. This article is an open access article distributed under the terms and conditions of the Creative Commons Attribution (CC BY) license (<https://creativecommons.org/licenses/by/4.0/>).

## 1. Introduction

The floral fragrance is an essential trait for plants to induce insect pollination, drive away herbivores or resist pathogens [1,2]. It is also critical for ornamental plants to positively affect people's health and mood through their pleasant scents [3]. Even though floral fragrance has important scientific and economic significance, flower-breeding goals used to be concentrated on flower color and shape, resulting in quite a few cultivated flowers have gradually lost their fragrance [4]. Thus, a growing body of research focusing on floral volatile compounds has been recently conducted in many fragrant plants.

At present, more than 2000 flower fragrance compounds of nearly 100 plant families have been identified [5]. Studies have shown that the main volatile compounds of the most famous economically important flower, *Rosa rugosa*, were phenethyl alcohol,  $\beta$ -citronellol and geraniol [1]. The key floral aroma constituents of *Osmanthus fragrans* [6], *Chimonanthus praecox* [7], camellias [8] and lilies [9], the most well-known fragrant flowers in China, all contain linalool. In addition, there were significant differences in the floral components of the different aromatic plant species, even among the different cultivars [10,11]. The distinct odors appear to act as different olfactory cues that guide insects to specific flowers.

There are many factors to be considered when investigating floral scents, including scent emission by oil secretory cells in different floral parts and how this varies according to flowering stages. Studies in many fragrant plants such as crabapple [12], *Luculia pinceana* [3] and *Cananga odorata* [13] have shown that the temporal patterns of odorant emission from flowers are comparable, while studies in *Protea* [14], *Hosta* [15] and *Dianthus inoxianus* [16]

have shown that there are usually a variety of spatial patterns. Moreover, the distribution of the oil cells in flower organs has a significant effect on floral scent production [17], as volatile compounds are synthesized in the oil cells and are immediately released and disperse [6,18].

*Michelia* L. is a large genus from the Magnoliaceae family commonly found in the temperate zone of India, China, Malaysia and Indonesia, consisting of about 80 tree- or shrub-habit species [19]. Species from the *Michelia* genus are widely used as ornamental plants and floral essential oil sources [17]. The types and contents of fragrant floral components in *M. alba* [20], *M. champaca* [21] and *M. compressa* var. *formosana* [22] also vary, with the major compounds being linalool, methyl benzoate,  $\beta$ -pinene, etc. *M. crassipes*, a great ornamental evergreen shrub from *Michelia*, is widely used in landscaping due to its pleasant fragrance and unique dark purple tepals amongst *Michelia* species [23]. It has become a highly desirable cross-breeding germplasm resource with a total of nine new *Michelia* interspecific hybrid varieties derived from *M. crassipes* in recent decades [17]. However, there have been no reports on the scent properties of the different flower organs of *M. crassipes* and their variation between different flowering stages.

In this study, we employed headspace solid-phase microextraction (HS-SPME) combined with gas chromatography high-resolution mass spectrometry (GC-HRMS) for the first time to identify the key scent compounds emitted from different parts of the *M. crassipes* flower at different flowering stages. The spatiotemporal variances of oil secretory cells in the *M. crassipes* flower were also observed by paraffin sections. These results provide a theoretical basis not only for the further exploration of *Michelia* species floral fragrance breeding and essential oil extraction development but also for studying spatiotemporal variances in scent emission concerning pollinator behavior.

## 2. Materials and Methods

### 2.1. Plant Materials and Sampling

The *M. crassipes* plants used in this paper were semi-naturally grown in a tree farm (unheated and natural photoperiod) of the Forestry Department of Hunan Province (Changsha, Hunan) [24]. Flowers from ten different five-year-old plant individuals with similar growth at the bud stage (S1), initial flowering stage (S2) and full flowering stage (S3) were collected at 9:00 a.m. on 4th May 2021 (Figure 1) in sunny weather without wind. A total of twelve flowers at each stage were collected into an ice box and instantly brought to the laboratory. The whole flower was divided into tepals, pistil and stamens by pointed tweezers and then utilized in the following experiments.



**Figure 1.** Typical samples of three flower development stages. S1: bud stage (length/cm  $1.786 \pm 0.016$  c, the buds were swollen with cracked bracts, and the purple tepals were exposed); S2:

initial flowering stage (length/cm  $2.059 \pm 0.049$  b, the flowers were about to open, and the male and female stamens were exposed, and the pollen was not scattered); S3: full flowering stage (length/cm  $2.444 \pm 0.033$  a, the inner and outer tepals were fully open, and the pollen was about to scatter). Different letters of flower length mean a significant difference  $p < 0.05$ .

## 2.2. HS-SPME Analysis

The separated and de-stalked flower samples (tepals, stamens and pistil) were first flushed with nitrogen and then crushed using a mixer mill (MM 400, Retsch) with a zirconia bead for 1.5 min at 30 Hz [17]. Then, 100 mg of powder was weighed and placed in a 20 mL solid-phase microextraction (SPME) bottle (Thermo Fisher Scientific, Waltham, MA, USA) with 1  $\mu$ L internal standard, a mixture of 10  $\mu$ L 4-methyl-2-pentanol (CAS#108-11-2,  $0.802 \mu\text{g}\cdot\text{kg}^{-1}$ , Sigma-Aldrich) dissolved in 990  $\mu$ L distilled water. Each sample was equilibrated at 60 °C in a water bath for 10 min before analysis. An SPME fiber coated with 50/30  $\mu\text{m}$  divinylbenzene/carboxen/polydimethylsiloxane (DVB/CAR/PDMS, Supelco, Bellefonte, PA) was exposed in the vial headspace for 40 min at 60 °C after equilibration. Then, the fiber was introduced into a GC injection port at 250 °C for a 3 min desorption.

## 2.3. GC-HRMS Analysis

The adsorbed volatiles was analyzed using GC-HRMS, performed using a Trace 1310 GC chromatograph equipped with a TriPlus RSH autosampler and coupled to a Q-Exactive Orbitrap mass analyzer (Thermo Fisher Scientific, Waltham, MA, USA) [25]. Chromatographic separation was performed on a DB-5MS capillary column (30 m  $\times$  0.25 mm, 0.25  $\mu\text{m}$  thickness; Agilent Technologies, Palo Alto, CA, USA). Helium (99.999%) was the carrier gas in the split mode with the split ratio at 5 and column flow at 1 mL  $\text{min}^{-1}$ . The GC oven temperature was programmed at 70 °C for a 1 min hold initially, and then to 100 °C at a rate of 12 °C  $\text{min}^{-1}$ , followed by 180 °C at a rate of 2 °C  $\text{min}^{-1}$  and 250 °C at a rate of 12 °C  $\text{min}^{-1}$  with a 2 min hold at the final temperature. HRMS acquisition was performed using electron ionization (EI) at 70 eV, and the full-scan MS mode was performed in a scan range of  $m/z$  30–300. Resolution power was set at 120,000 full widths at half-maximum ( $m/z$  200), mass error  $\leq 1$  ppm. Ion source and MS transfer line temperatures were set at 250 °C.

## 2.4. Data Analysis

Compounds were identified by matching the mass spectra with the NIST 11 library (the National Institute of Standards and Technology 2011, Shimadzu, Japan) by the TraceFinder software (Thermo Fisher Scientific) with a similarity more than 90%. Quantification data were confirmed by standardizing the peak area of each component with the internal standard. The mass fraction was calculated using the following formula [26]: compound emission amount ( $\mu\text{g}\cdot\text{kg}^{-1}$ ) = peak area of compound  $\times$  internal standard mass ( $\mu\text{g}$ )  $\times$  relative molecular mass of compound/peak area of internal standard  $\times$  sample mass (g). The odor activity values (OAVs) were computed by dividing the calculated concentrations with literature sensory thresholds in water [27]. Odor description terms of fresh flowers were derived by referring to the Odor Detection Thresholds & References, The Good Scents Company Search Page and Flavornet databases. OriginPro 2022 (<https://www.originlab.com> accessed on 8 August 2022) was used for principal component analysis, the calculation of the eigenvector load value, and the study of the leading components. TBtools (Toolbox for Biologists) was used to perform the Venn diagram analysis and hierarchical cluster analysis of the data [28]. The results were expressed as the mean value and standard deviation (mean  $\pm$  SD) for five replicates.

## 2.5. Paraffin Section Detection

Fresh tepals, pistil and stamens of *M. crassipes* were fixed in formaldehyde–alcohol–acetic acid (FAA) fixative and then dehydrated by application of an alcohol gradient. After dehydration, the alcohol was gradually replaced with the xylene (2/3 alcohol + 1/3 xylene,

1/3 alcohol + 2/3 xylene, 20 min each step; xylene, xylene, 10 min each step) for transparency [29]. The samples were then embedded in paraffin, and the sections were obtained using a RM2235 microtome (Leica, Wetzlar, German). The paraffin sections were stained with fast green (1%, w/w) and safranin (1%, w/w), and then observed and photographed using an Olympus DP71 microscope (Olympus, Tokyo, Japan).

### 3. Results

#### 3.1. Volatile Compounds Identification in *M. crassipes* Flower

The HS-SPME and GC-Orbitrap-HRMS system was used to gain insights into the constitution of *M. crassipes* floral volatiles. The peak area of every compound was integrated to obtain the total ion current (Figure S1). The detected chromatographic peaks and retention indices were then subjected to spectrum library retrieval. By filtering compounds accounting for less than 0.01% of the total amount, 69 compounds were identified as flower scent compounds according to the descriptions [5,10,30] (Table S1). The main chemical categories were terpene (48), alcohol (11), ester (5), benzenoid (3), aldehyde (3), phenol (1) and ketone (1), among which terpenes were the most abundant in every profile, accounting for up to 84% of the total (Table 1).

**Table 1.** Relative content of flower scent compounds of *M. crassipes* by chemical category. (T: tepals; S: stamens; P: pistil; S1: bud stage; S2: initial flowering stage; S3: full flowering stage; values are mean  $\pm$  SD of five replicates).

Category	Relative Content (%)								
	T-S1	T-S2	T-S3	S-S1	S-S2	S-S3	P-S1	P-S2	P-S3
terpene	71.8 $\pm$ 3.54	72.06 $\pm$ 3.56	74.16 $\pm$ 3.68	70.24 $\pm$ 3.47	65.17 $\pm$ 3.23	74.5 $\pm$ 3.69	78.58 $\pm$ 3.87	76.16 $\pm$ 3.73	83.87 $\pm$ 4.13
alcohol	4.12 $\pm$ 0.2	3.1 $\pm$ 0.16	2.37 $\pm$ 0.12	7.23 $\pm$ 0.36	7.66 $\pm$ 0.38	4.63 $\pm$ 0.22	1.71 $\pm$ 0.08	1.63 $\pm$ 0.08	1.58 $\pm$ 0.06
ester	0.65 $\pm$ 0.03	1.64 $\pm$ 0.09	1.23 $\pm$ 0.07	1.96 $\pm$ 0.1	2.23 $\pm$ 0.11	1.47 $\pm$ 0.08	0.36 $\pm$ 0.02	3.46 $\pm$ 0.17	0.35 $\pm$ 0.01
benzenoid	0.7 $\pm$ 0.03	0.66 $\pm$ 0.04	0.44 $\pm$ 0.02	6.61 $\pm$ 0.33	6.73 $\pm$ 0.33	3.68 $\pm$ 0.18	0.51 $\pm$ 0.03	0.51 $\pm$ 0.03	0.52 $\pm$ 0.02
aldehyde	0.05 $\pm$ 0	0.05 $\pm$ 0	Tr	0.2 $\pm$ 0.01	0.55 $\pm$ 0.03	0.21 $\pm$ 0.01	0.15 $\pm$ 0	0.16 $\pm$ 0	0.15 $\pm$ 0
phenol	Tr	Tr	0.17 $\pm$ 0.01	Tr	Tr	0.14 $\pm$ 0.01	0.17 $\pm$ 0.01	Tr	0.12 $\pm$ 0.01
ketone	Tr	Tr	Tr	Tr	Tr	Tr	0.04 $\pm$ 0	0.04 $\pm$ 0	0.04 $\pm$ 0

Tr: trace, less than 0.01.

Figure 2 shows that twenty-four floral scent compounds represented more than 1% of the total emission from each floral parts at different flowering stages. Among them,  $\alpha$ -guaiene was the most abundant, with amounts ranging from 15.32% to 51.06%, followed by  $\beta$ -caryophyllene (7.03–16.49%) and germacrene B (6.96–14.04%). Moreover,  $\beta$ -humulene (2.89–4.86%),  $\alpha$ -caryophyllene (2.35–3.43%),  $\gamma$ -muurolene (3.32–5.89%) and  $\alpha$ -copaene (1.86–3.87%) also constituted a large percentage of the total amount from each floral part at different flowering stages.

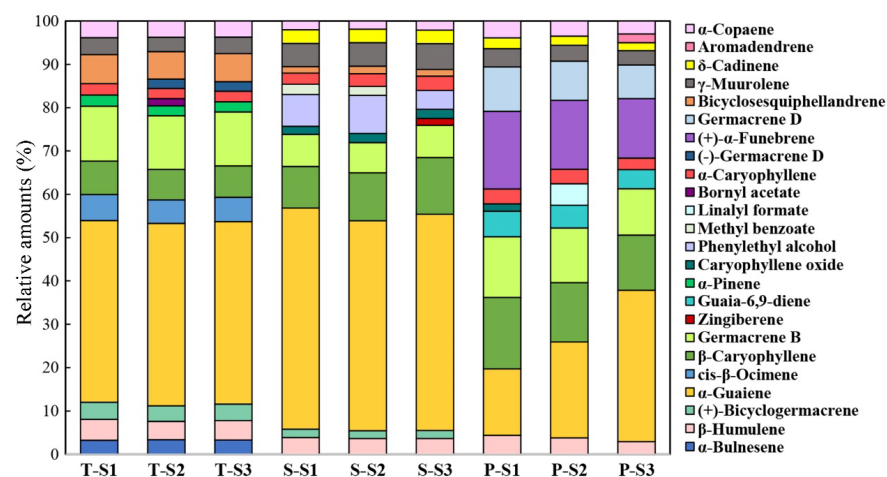


**Figure 2.** Major components (>1%) of floral volatiles emitted from *M. crassipes*. (T: tepals; S: stamens; P: pistil; S1: bud stage; S2: initial flowering stage; S3: full flowering stage).

The aroma or odor activity value (OAV) is frequently used to confirm which aroma compounds are key to an overall flavor extract [31]. The OAVs were calculated by dividing the averages of analytical concentrations with published odor thresholds [27]. Typically, floral volatiles with high OAVs (>1) are more likely to be the main contributors to flower fragrance, while the ones with OAVs between 1 and 0.1 have less contribution. When the OAV values are below 0.1, the volatiles might not contribute to floral fragrance. Therefore, the fourteen compounds in Table 2 are listed in terms of decreasing OAVs (>0.1) for the different floral parts of *M. crassipes* at the three flowering stages (S1, S2 and S3), and seven of them had an OAV greater than 1.

**Table 2.** Volatile components with odor activity values more than 0.1 (OAVs > 0.1) in *M. crassipes* flowers. (T: tepals; S: stamens; P: pistil; S1: bud stage; S2: initial flowering stage; S3: full flowering stage).

Compound	RT	Odor Threshold *	Odor Description * <sup>2</sup>	OAVs								
				T-S1	T-S2	T-S3	S-S1	S-S2	S-S3	P-S1	P-S2	P-S3
Ethyl 3-methyl valerate	18.084	0.008	fruit, pineapple	0.29	0.01	0.16	15.66	31.30	28.00	20.99	32.64	33.22
Methyl benzoate	9.071	0.52	fruit, sweet	2.15	1.60	1.70	6.00	7.48	4.50	2.94	3.78	4.06
$\beta$ -Damascone	42.968	0.009	fruit, berry	Tr * <sup>3</sup>	Tr	Tr	Tr	Tr	Tr	2.92	3.73	4.00
$\beta$ -Caryophyllene	29.443	64	wood, pepper	0.41	0.45	0.48	0.20	0.33	0.45	2.20	2.54	2.87
$\alpha$ -Pinene	32.331	6	wood, pine	1.44	1.52	1.64	0.23	0.40	0.52	1.69	1.91	2.40
$\beta$ -Ionone	45.309	0.1	flower, iris	Tr	1.20	1.29	Tr	Tr	Tr	Tr	Tr	Tr
Phenylethyl alcohol	13.697	15	flower, rose	0.16	0.21	0.13	0.64	1.11	0.64	0.37	0.51	0.60
Butanal	6.049	2	spice, cocoa	Tr	0.15	Tr	0.12	0.38	Tr	0.46	0.73	0.66
Benzyl acetate	30.737	2	sweet, jasmine	Tr	Tr	0.66	Tr	0.05	0.06	0.02	0.02	0.01
<i>cis</i> - $\beta$ -Ocimene	29.388	34	flower, nasturtium	0.60	0.64	0.69	0.01	0.01	0.02	0.02	0.03	0.03
Linalool	12.978	6	flower, rose	0.40	0.42	0.35	Tr	Tr	Tr	Tr	Tr	Tr
$\beta$ -Selinene	31.489	1	herb	Tr	0.25	0.34	Tr	Tr	Tr	Tr	Tr	Tr
Bornyl acetate	21.698	75	wood, mint	Tr	Tr	0.08	0.31	0.06	0.14	0.15	0.05	0.14
$\alpha$ -Caryophyllene	31.388	160	wood, lilac	0.06	0.06	0.06	0.02	0.04	0.05	0.18	0.25	0.24
D-Limonene	10.823	10	green, lemon	0.05	0.06	0.07	0.01	Tr	0.04	0.18	0.21	0.22
Nerolidol	36.983	15	flower, citrus	0.19	0.21	0.19	0.02	0.03	0.05	Tr	Tr	0.05

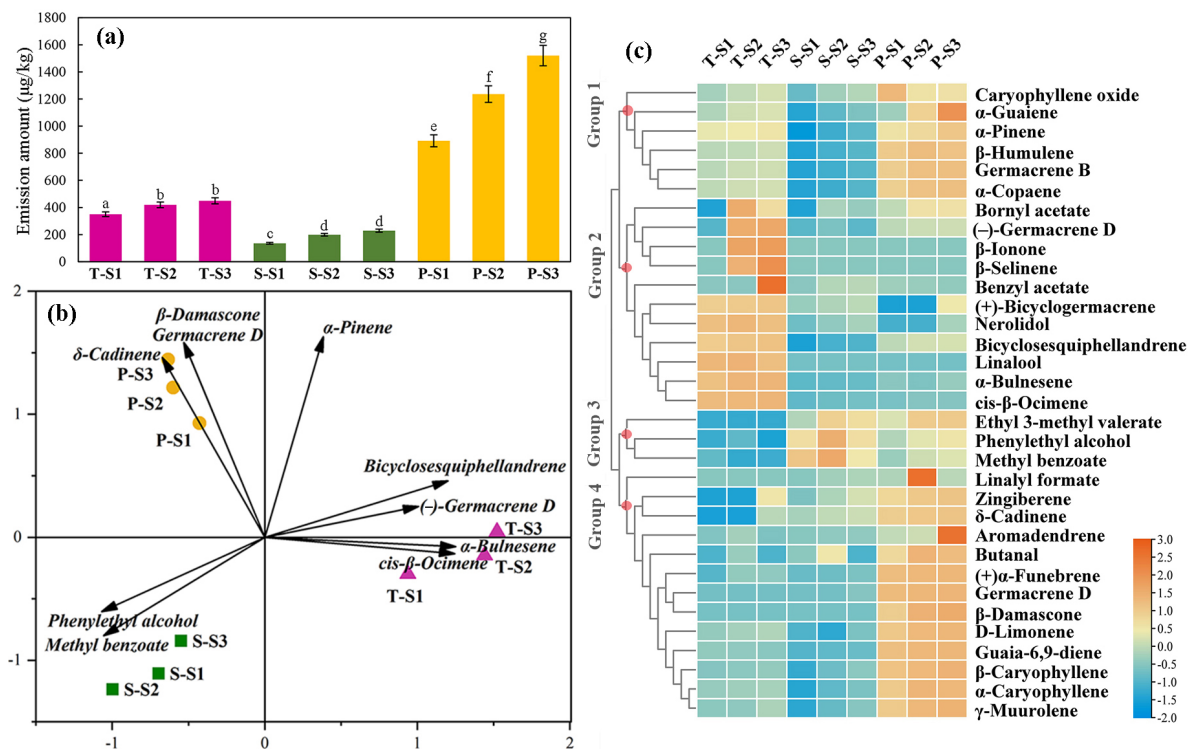
\* OAV values are calculated based on literature thresholds. \*<sup>2</sup> Excerpts from the Odor Detection Thresholds & References, The Good Scents Company Search Page and Flavournet databases. RT: Retention Time (min). \*<sup>3</sup> Tr: trace, less than 0.01.

Ethyl 3-methyl valerate (fruity odor like pineapple), methyl benzoate (fruity and sweet odor),  $\beta$ -damascone (fruity odor like berry),  $\beta$ -caryophyllene (woody odor like pepper),  $\alpha$ -pinene (woody odor like pine),  $\beta$ -ionone (floral odor like iris) and phenylethyl alcohol (floral odor like rose) with high OAVs (>1) were considered to be the main characteristic aroma compounds of *M. crassipes* flowers, which are potent odorants present at low levels. On the other hand, *cis*- $\beta$ -ocimene,  $\alpha$ -caryophyllene and bornyl acetate with relative contents more than 1% had OAVs below one might have less of a contribution to the floral and woody fragrance of *M. crassipes*. Apart from that shown in Table 2, we cannot assess the OAVs of other main volatiles shown in Figure 2 since no odor thresholds were available. Therefore, the volatiles that represented less than 1% of the total emission but possessed an OAV > 0.1 were additionally considered to be the main floral volatiles of *M. crassipes*, including ethyl 3-methyl valerate,  $\beta$ -damascone,  $\beta$ -ionone,  $\beta$ -selinene, D-limonene and nerolidol with relative amounts below 0.1%.

### 3.2. Temporal and Spatial Patterns of Scent Emission in *M. crassipes* Flowers

A comparison of the major volatile compounds in different floral parts and different flowering stages was performed to explore the spatiotemporal variation of aroma emission. Figure 3a showed that volatile components were most abundant in the pistil with an overall increase in emission across flowering stages (891.82–1520.63  $\mu$ g/kg), which was approximately three- and seven-fold that of tepals (350.12–449.11  $\mu$ g/kg) and stamens (135.72–229.05  $\mu$ g/kg), respectively. By hierarchical cluster analysis, the compounds with similar emission patterns were mainly clustered into four groups (Figure 3b). Compounds

clustered in Groups 1 and 4 had relatively high emission amounts from the pistil, while compounds grouped in Groups 2 and 3 were mainly released from the tepals and stamens, respectively. Among them, opened flowers elicited a marked increase in  $\alpha$ -guaiene, linalyl formate and aromadendrene in the pistil, bornyl acetate, (-)-germacrene D,  $\beta$ -ionone,  $\beta$ -selinene and benzyl acetate in the tepals, and methyl benzoate and phenylethyl alcohol in the stamens.



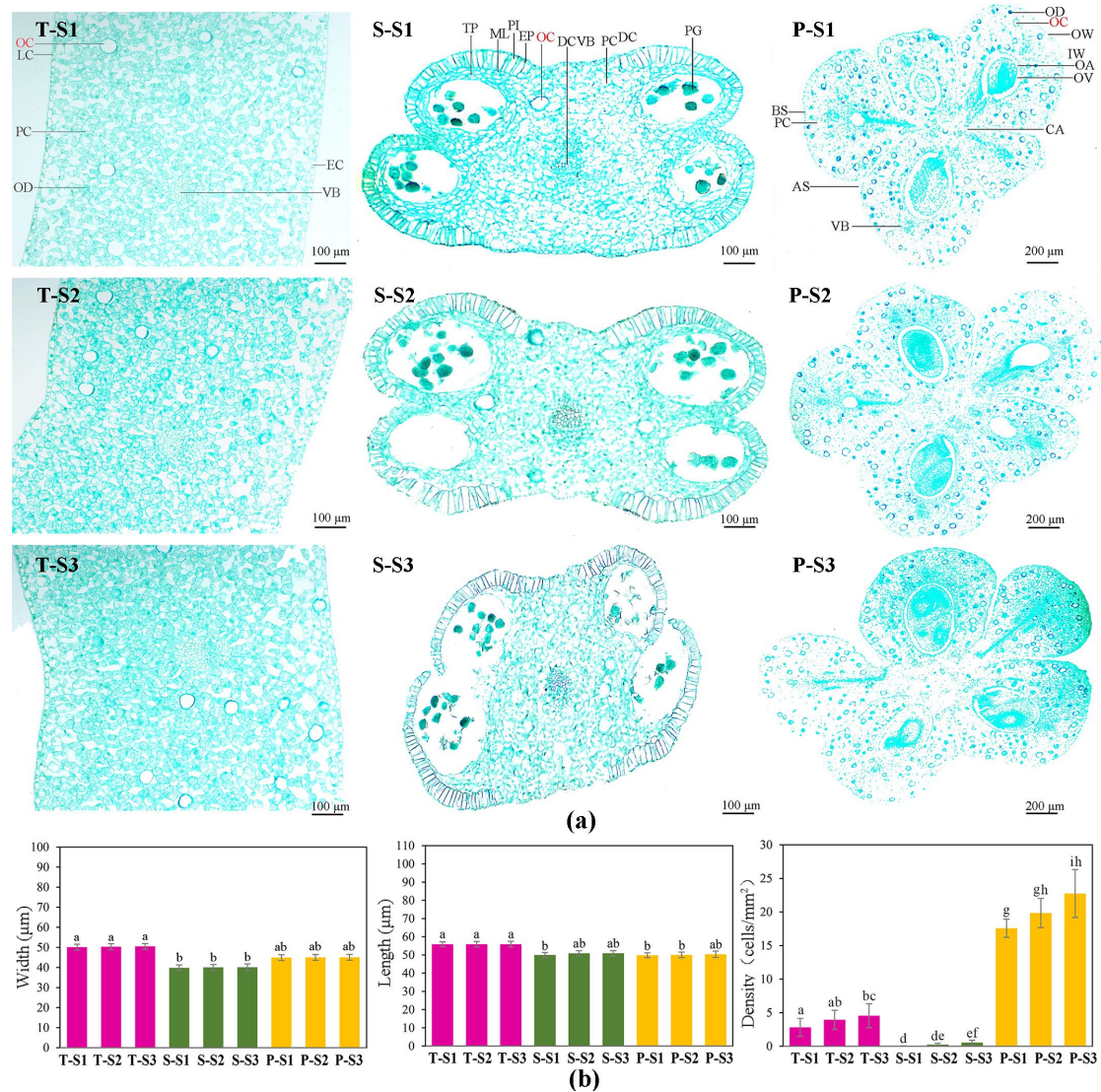
**Figure 3.** Spatiotemporal analysis (a), heatmap and hierarchical cluster analysis (b) and principal component analysis (c) of the emission amounts of the main floral aroma compounds of *M. crassipes*. Values are mean  $\pm$  SD of three replicates. Different letters of flower length indicate a significant difference ( $p < 0.05$ ). (T: tepals; S: stamens; P: pistil; S1: bud stage; S2: initial flowering stage; S3: full flowering stage).

Figure 3c presents the principal component analysis of the major volatile compounds in different floral parts and at different flowering stages. The variances of PC1 and PC2 were 56.2% and 36.3%, respectively. The ten highest loading values in each PC were chosen as the main factors contributing to separating the three floral parts.  $\delta$ -Cadinene,  $\beta$ -damascone and germacrene D were the main compounds distinguishing the pistil from tepals and stamens. Bicyclosesquiphellandrene, (-)-germacrene D,  $\alpha$ -bulnesene and *cis*- $\beta$ -ocimene helped to separate the tepals from the other parts, while  $\alpha$ -pinene helped to separate tepals and pistil from stamens. Additionally, methyl benzoate and phenylethyl alcohol were the principal compounds that distinguished stamens from the other parts. However, samples in the same floral part from different flowering stages did not show major differences.

### 3.3. Oil Cells in Different Floral Parts of *M. crassipes* at Different Flowering Stages

In Magnoliaceae species, the aroma volatiles are mainly produced in the floral parts, i.e., tepals, stamens and pistil, in specialized oil cells [17]. To test the role of oil cells in determining the aroma emission from *M. crassipes* flowers, paraffin sectioning was carried out with different floral parts at the three stages of flowering. The cross-sections showed the oil cells were distributed in the basic parenchyma of the tepals, pistil and stamens (Figure 4a). The size of the oil cells ranged from 39.79 to 55.89  $\mu$ m and did not show distinct variances between different floral parts and different flowering stages. However, these oil

cells were significantly denser in flowers than in buds, and denser in pistil than in tepals and stamens (Figure 4b). By Pearson correlation analysis, we found the variances of oil cells were positively correlated with the total emission amounts of the flower aroma compounds ( $r = 0.98$ ) of *M. crassipes*.



**Figure 4.** Cross-sections of *M. crassipes* flower organs (a) and comparison of their oil cells (b) at three flowering stages. Values are mean  $\pm$  SD of three replicates. Different letters indicate a significant difference ( $p < 0.05$ ). (T: tepals; S: stamens; P: pistil; S1: bud stage; S2: initial flowering stage; S3: full flowering stage; EP: epidermis; DCVB: drug compartment vascular bundle; PI: pharmacy interior; ML: middle layer; TP: tapetum; FL: fiber layer; PG: pollen grains; PC: parenchyma cells; OC: oil cells; OD: oil droplets; DC: drug compartment).

## 4. Discussion

### 4.1. Floral Aroma Characteristics of *M. crassipes*

Species from the *Michelia* genus are among the most well-known fragrant flowers throughout subtropical and tropical areas. The floral scent composition usually differs among species of a given genus [5]. The studies of volatile compounds of some *Michelia* flowers showed that the main volatile constituents are methyl benzoate in *M. compressa* [32], isobutyl acetate in *M. figo* [33], and methyl benzoate, indole and 1,8-cineole in *M. champaca* [21], etc. The method of solid-phase microextraction (SPME) from the static headspace (HS) of flower samples is the current mainstream method for determining flower volatiles.

This method is straightforward and sensitive for collecting the volatiles which can be subsequently analyzed by a gas chromatography and mass spectrometry (GC-MS) system [8,12]. Meanwhile, a high-resolution mass spectrometry analyzer (HRMS), such as Orbitrap one, has the advantage of providing mass acquisition for the reliable identification of compounds at very low concentrations [25]. To date, the HS-SPME coupled with GC-HRMS has been used in several studies of volatile organic compounds in wines and foods [34,35]. In this study, HS-SPME-GC-Orbitrap-HRMS was used in floral volatiles analysis to identify more abundant compounds including potent aroma volatiles present at trace levels. Our results showed that the main compounds of *M. crassipes* flower are terpenes, including 48 compounds representing a total relative content of up to 84%.  $\alpha$ -Guaiene,  $\beta$ -caryophyllene and germacrene B belonging to terpenes had the highest relative contents.

Many floral volatiles present at negligible levels were also identified using GC combined with HRMS, which usually could not be identified due to chromatographic coelution of interfering substances and low signal-to-noise ratios [25]. OAV values were used to determine the contribution of each compound to floral fragrance traits. A total of 16 compounds with an OAV greater than 0.1 were considered to be the main characteristic aroma compounds, which can be described as fruity, woody and floral odors. Among them, ethyl 3-methyl valerate, methyl benzoate and  $\beta$ -damascone had the highest OAVs, which are likely to be the main contributors to the fruity odor of *M. crassipes* flowers. This result is consistent with the previous hypothesis that beetle-pollinated flowers, such as Magnoliaceae species, mimic fruit odors [14]. It is possible that *M. crassipes* evolved specialist fruity scents dominated by ethyl 3-methyl valerate, methyl benzoate and  $\beta$ -damascone to attract beetle pollinators.

However, owing to the limitations of the OAV approach, the contribution of quite a few compounds to *M. crassipes* floral aroma still cannot be determined, since their odor thresholds are unknown. Meanwhile, the odor description of floral volatiles was limited as well. It is beneficial to characterize the floral aroma profiles of *M. crassipes* by using gas chromatography-olfactometry (GC-O) and human sensory evaluation [27]. On the other hand, HS-SPME is an analytical extraction technique that depends on the affinity of the components of the volatiles relative to the fiber used. As a result, the composition of the volatiles emitted by *M. crassipes* may be different from the actual composition since only compounds with affinity to the fiber used have been characterized. These problems will be studied further. In general, the scent of *M. crassipes* is different from other famous fragrant flowers, like Rosaceae flowers [1,36], whose fragrance is simply derived from a couple of high-content compounds.

#### 4.2. Spatiotemporal Variation of Floral Scent of *M. crassipes*

Spatiotemporal variation in floral scent emission has biological significance in mediating pollinator attractiveness [14]. Flowers usually start to produce fragrance when they are ready to spread and receive pollen to maximize pollination opportunities [3,12,13,37]. This seemed to occur in *M. crassipes* as well, as emitted scent components were drastically increased at the stage of full bloom in all isolated floral parts. However, the pistil emitted a much higher abundance of odorant components than the tepals and stamens of *M. crassipes*, which contrasts with the findings from many other species [14–16]. This can be explained by the distribution variances of specialized oil cells in *M. crassipes* flowers, where the aroma volatiles are mainly produced. The oil cells of a similar size were scattered throughout the tepals, stamens and pistil in *M. crassipes*, but were much more densely packed in the pistil compared to the tepals and stamens. In contrast, oil cell density in *Magnolia zenii* has been shown to be greatest in the tepals [38]. Meanwhile, the density of oil cells in *M. crassipes* flowers also increased along with flowering, which was consistent with findings from *Magnolia sirindhorniae* [17]. Furthermore, it would be of great interest to further investigate whether volatile emission is dependent on floral transpiration across cultivars or species, as cases in which transpiration of flowers exceeds that of leaves have been reported [39].

Usually, tepals are the source of floral scents, but distinct pollinator attractants can also be emitted by pollen [40] or nectar [14,16]. Similar nectar odors were detected in different species, giving rise to a shared signal to pollinators, whereas differences between odors of other flower organs, e.g., bracts, perianths and styles reflect species differences [14,16]. Instead of nectar, the beetle-pollinated flowers of Magnoliaceae species produce large quantities of pollen that the beetles use for food for pollinator attractiveness. Here, we found the stamens in *M. crassipes* seemed to be responsible for emitting the benzenoids, including methyl benzoate and phenylethyl alcohol, at the stage of initial blooming. This could facilitate pollinator orientation to *M. crassipes* pollen, because the benzenoids have proven to be an ‘honest signal’ of a reward to a pollinator [41,42]. On the other hand, the scent of the other floral parts was characterized by terpenes such as  $\delta$ -cadinene,  $\beta$ -damascone germacrene D,  $\alpha$ -bulnesene and *cis*- $\beta$ -ocimene, which are a source of natural antioxidants and antimicrobial agents [17].

## 5. Conclusions

The major floral scent compounds in *M. crassipes* were  $\alpha$ -guaiene,  $\beta$ -caryophyllene and germacrene B with high relative contents, as well as ethyl 3-methyl valerate, methyl benzoate and  $\beta$ -damascone with high OAV values. These compounds contribute to complex fruity, woody and floral aromas, which are strongly emitted in the pistil followed by the tepals and stamens at the stage of full flowering. This spatiotemporal variation in scent emission is correlated with the changes in oil cell density in different floral parts and different flowering stages. The methyl benzoate and phenylethyl alcohol emitted distinctly from stamens might act as a cue to pollinators of *M. crassipes*.

The GC-HRMS methodology combined with HS-SPME, which has been performed for the first time in this study, could be applicable for determining the complicated floral volatiles of *M. crassipes*. It would also be of great practical interest to compare the composition of volatiles and essential oils from different floral organs by HS-SPME. These results encourage the implementation of this untargeted metabolomics approach in the field of identification and quantification of volatile organic compounds from other fragrant flowers.

**Supplementary Materials:** The following supporting information can be downloaded at: <https://www.mdpi.com/article/10.3390/horticulturae9040442/s1>, Figure S1: Total ion chromatograms (TICs) of volatile components of different flower organs of *M. crassipes* at three flowering stages (S1, S2 and S3); Table S1: Emission amounts of 69 different floral volatiles detected in *M. crassipes* flowers in the tepals (T), pistil (P) and stamens (S) at three flowering stages (S1, S2 and S3).

**Author Contributions:** Conceptualization, X.J. and J.Y.; methodology, X.J. and J.Y.; software, Y.Y.; validation, Z.Z., Y.C. and M.Z.; formal analysis, Y.Y.; investigation, J.Y.; writing—original draft preparation, Y.Y.; writing—review and editing, Y.Y.; project administration, X.J.; funding acquisition, X.J. and Y.H.; Y.Y. and J.Y. contribute equally to the article. All authors have read and agreed to the published version of the manuscript.

**Funding:** This research was funded by the Research Foundation of the Education Bureau of Hunan Province, China (outstanding young talents project: 22B0259).

**Data Availability Statement:** Not applicable.

**Acknowledgments:** The authors thank Lihong Yan of the Institute of Plant Conservation and Utilization of Hunan Botanical Garden for his contribution to the identification of the plant material.

**Conflicts of Interest:** The authors declare no conflict of interest.

## References

1. Feng, D.; Zhang, H.; Qiu, X.; Jian, H.; Wang, Q.; Zhou, N.; Ye, Y.; Lu, J.; Yan, H.; Tang, K. Comparative transcriptomic and metabolomic analysis revealed the relationships between biosynthesis of volatiles and flavonoid metabolites in *Rosa rugosa*. *Ornam. Plant. Res.* **2021**, *1*, 5. [CrossRef]
2. Meng, L.; Shi, R.; Wang, Q.; Wang, S. Analysis of floral fragrance compounds of *Chimonanthus praecox* with different floral colors in Yunnan, China. *Separations* **2021**, *8*, 122. [CrossRef]

3. Li, Y.; Ma, H.; Wan, Y.; Li, T.; Liu, X.; Sun, Z.; Li, Z. Volatile organic compounds emissions from *Luculia pinceana* flower and its changes at different stages of flower development. *Molecules* **2016**, *21*, 531. [[CrossRef](#)] [[PubMed](#)]
4. Dudareva, N.; Negre, F.; Nagegowda, D.A.; Orlova, I. Plant volatiles: Recent advances and future perspectives. *Crit. Rev. Plant Sci.* **2006**, *25*, 417–440. [[CrossRef](#)]
5. Knudsen, J.T.; Eriksson, R.; Gershenzon, J.; Ståhl, B. Diversity and distribution of floral scent. *Bot. Rev.* **2006**, *72*, 1. [[CrossRef](#)]
6. Han, Y.; Wang, H.; Wang, X.; Li, K.; Dong, M.; Li, Y.; Zhu, Q.; Shang, F. Mechanism of floral scent production in *Osmanthus fragrans* and the production and regulation of its key floral constituents,  $\beta$ -ionone and linalool. *Hortic. Res.* **2019**, *6*, 106. [[CrossRef](#)]
7. Tian, J.; Ma, Z.; Zhao, K.; Zhang, J.; Xiang, L.; Chen, L. Transcriptomic and proteomic approaches to explore the differences in monoterpene and benzenoid biosynthesis between scented and unscented genotypes of wintersweet. *Physiol. Plant* **2019**, *166*, 478–493. [[CrossRef](#)]
8. Fan, Z.; Li, J.; Li, X.; Yin, H. Composition analysis of floral scent within genus *Camellia* uncovers substantial interspecific variations. *Sci. Hortic.* **2019**, *250*, 207–213. [[CrossRef](#)]
9. Kong, Y.; Bai, J.; Lang, L.; Bao, F.; Dou, X.; Wang, H.; Shang, H. Variation in floral scent compositions of different lily hybrid groups. *J. Am. Soc. Hortic. Sci.* **2017**, *142*, 175–183. [[CrossRef](#)]
10. Oyama-Okubo, N.; Tsuji, T. Analysis of floral scent compounds and classification by scent quality in tulip cultivars. *J. Jpn. Soc. Hortic. Sci.* **2013**, *82*, 344–353. [[CrossRef](#)]
11. Zhang, T.; Bao, F.; Yang, Y.; Hu, L.; Ding, A.; Wang, J.; Cheng, T.; Zhang, Q. A comparative analysis of floral scent compounds in intraspecific cultivars of *Prunus mume* with different corolla colours. *Molecules* **2019**, *25*, 145. [[CrossRef](#)] [[PubMed](#)]
12. Fan, J.; Zhang, W.; Zhang, D.; Wang, G.; Cao, F. Flowering stage and daytime affect scent emission of *Malus ioensis* “Prairie Rose”. *Molecules* **2019**, *24*, 2356. [[CrossRef](#)] [[PubMed](#)]
13. Qin, X.W.; Hao, C.Y.; He, S.Z.; Wu, G.; Tan, L.H.; Xu, F.; Hu, R.S. Volatile organic compound emissions from different stages of *Cananga odorata* flower development. *Molecules* **2014**, *19*, 8965–8980. [[CrossRef](#)]
14. Steenhuisen, S.L.; Raguso, R.A.; Jürgens, A.; Johnson, S.D. Variation in scent emission among floral parts and inflorescence developmental stages in beetle-pollinated *Protea* species (*Proteaceae*). *S. Afr. J. Bot.* **2010**, *76*, 779–787. [[CrossRef](#)]
15. Liu, Q.; Sun, G.; Wang, S.; Lin, Q.; Zhang, J.; Li, X. Analysis of the variation in scent components of *Hosta* flowers by HS-SPME and GC-MS. *Sci. Hortic.* **2014**, *175*, 57–67. [[CrossRef](#)]
16. Balao, F.; Herrera, J.; Talavera, S.; Dotterl, S. Spatial and temporal patterns of floral scent emission in *Dianthus innoxianus* and electroantennographic responses of its hawkmoth pollinator. *Phytochemistry* **2011**, *72*, 601–609. [[CrossRef](#)]
17. Ghosh, D.; Chaudhary, N.; Uma Kumari, K.; Singh, J.; Tripathi, P.; Meena, A.; Luqman, S.; Yadav, A.; Chanotiya, C.S.; Pandey, G.; et al. Diversity of essential oil-secretory cells and oil composition in flowers and buds of *Magnolia sirindhorniae* and its biological activities. *Chem. Biodivers.* **2021**, *18*, e2000750. [[CrossRef](#)]
18. Hadacek, F.; Weber, M. Club-shaped organs as additional osmophores within the *Sauromatum* inflorescence: Odour analysis, ultrastructural changes and pollination aspects. *Plant Biol.* **2002**, *4*, 367–383. [[CrossRef](#)]
19. Xu, H.; Li, F.; Pan, Y.; Gong, X. Interspecific hybridization processes between *Michelia yunnanensis* and *M. crassipes* and embryogenesis of the heterozygote. *HortScience* **2017**, *52*, 1043–1047. [[CrossRef](#)]
20. Cheng, K.K.; Nadri, M.H.; Othman, N.Z.; Rashid, S.; Lim, Y.C.; Leong, H.Y. Phytochemistry, bioactivities and traditional uses of *Michelia*  $\times$  *alba*. *Molecules* **2022**, *27*, 3450. [[CrossRef](#)]
21. Báeza, D.; Morales, D.; Pinob, J.A. Volatiles from *Michelia champaca* flower: Comparative analysis by simultaneous distillation-extraction and solid phase microextraction. *Nat. Prod. Commun.* **2012**, *7*, 659–660. [[CrossRef](#)]
22. Lesueur, D.; Serra, D.d.R.; Bighelli, A.; Hoi, T.M.; Ban, N.K.; Thai, T.H.; Casanova, J. Chemical composition and antibacterial activity of the essential oil of *Michelia foveolata* Merryll ex Dandy from Vietnam. *Flavour Fragr. J.* **2007**, *22*, 317–321. [[CrossRef](#)]
23. Chen, C.Y.; Kao, C.L.; Chen, H.C.; Huang, M.H.; Li, H.T.; Wu, M.D.; Cheng, M.J. A morpholine dimer of *Michelia crassipes*. *Chem. Nat. Compd.* **2021**, *57*, 468–470. [[CrossRef](#)]
24. Liu, C.; Yu, Q.; Li, Z.; Jin, X.; Xing, W. Metabolic and transcriptomic analysis related to flavonoid biosynthesis during the color formation of *Michelia crassipes* tepal. *Plant Physiol. Biochem.* **2020**, *155*, 938–951. [[CrossRef](#)] [[PubMed](#)]
25. Rivera-Perez, A.; Romero-Gonzalez, R.; Garrido Frenich, A. Feasibility of applying untargeted metabolomics with GC-Orbitrap-HRMS and chemometrics for authentication of black pepper (*Piper nigrum* L.) and identification of geographical and processing markers. *J. Agric. Food Chem.* **2021**, *69*, 5547–5558. [[CrossRef](#)]
26. Shi, S.; Duan, G.; Li, D.; Wu, J.; Liu, X.; Hong, B.; Yi, M.; Zhang, Z. Two-dimensional analysis provides molecular insight into flower scent of *Lilium* ‘Siberia’. *Sci. Rep.* **2018**, *8*, 5352. [[CrossRef](#)]
27. Du, X.; Plotto, A.; Baldwin, E.; Rouseff, R. Evaluation of volatiles from two subtropical strawberry cultivars using GC-olfactometry, GC-MS odor activity values, and sensory analysis. *J. Agric. Food Chem.* **2011**, *59*, 12569–12577. [[CrossRef](#)]
28. Chen, C.; Chen, H.; Zhang, Y.; Thomas, H.R.; Frank, M.H.; He, Y.; Xia, R. TBtools—An integrative toolkit developed for interactive analyses of big biological data. *Mol. Plant* **2020**, *13*, 1194–1202. [[CrossRef](#)]
29. Gao, H. The Forming and Releasing and Chemical Components of Fragrance of Three Species in *Michelia* Linn. Master’s Thesis, Fujian Agriculture and Forestry University, Fuzhou, China, 2009.
30. Muhlemann, J.K.; Klempien, A.; Dudareva, N. Floral volatiles: From biosynthesis to function. *Plant Cell Environ.* **2014**, *37*, 1936–1949. [[CrossRef](#)]

31. Methven, L. Techniques in sensory analysis of flavour. In *Flavour Development, Analysis and Perception in Food and Beverages*; Parker, J.K., Elmore, J.S., Methven, L., Eds.; Woodhead Publishing: Cambridge, UK, 2015; pp. 353–368. [\[CrossRef\]](#)
32. Azuma, H.; Toyota, M.; Asakawa, Y.; Yamaoka, R.; García-Franco, J.G.; Dieringer, G.; Thien, L.B.; Kawano, S. Chemical divergence in floral scents of magnolia and allied genera (*Magnoliaceae*). *Plant Species Biol.* **1997**, *12*, 69–83. [\[CrossRef\]](#)
33. Azuma, H.; Thien, L.B.; Kawano, S. Floral scents, leaf volatiles and thermogenic flowers in *Magnoliaceae*. *Plant Species Biol.* **1999**, *14*, 121–127. [\[CrossRef\]](#)
34. Liu, Y.; Qian, X.; Xing, J.; Li, N.; Li, J.; Su, Q.; Chen, Y.; Zhang, B.; Zhu, B. Accurate Determination of 12 Lactones and 11 Volatile Phenols in Nongrape Wines through Headspace-Solid-Phase Microextraction (HS-SPME) Combined with High-Resolution Gas Chromatography-Orbitrap Mass Spectrometry (GC-Orbitrap-MS). *J. Agric. Food Chem.* **2022**, *70*, 1971–1983. [\[CrossRef\]](#) [\[PubMed\]](#)
35. Romera-Torres, A.; Arrebola-Liébanas, J.; Vidal, J.L.M.; Frenich, A.G. Determination of Calystegines in Several Tomato Varieties Based on GC-Q-Orbitrap Analysis and Their Classification by ANOVA. *J. Agric. Food Chem.* **2019**, *67*, 1284–1291. [\[CrossRef\]](#)
36. Scalliet, G.; Piola, F.; Douady, C.J.; Réty, S.; Raymond, O.; Baudino, S.; Bordji, K.; Bendahmane, M.; Dumas, C.; Cock, J.M.; et al. Scent evolution in Chinese roses. *Proc. Natl. Acad. Sci. USA* **2008**, *105*, 5927–5932. [\[CrossRef\]](#)
37. Dudareva, N.; Pichersky, E. Biochemical and molecular genetic aspects of floral scents. *Plant Physiol.* **2000**, *122*, 627–633. [\[CrossRef\]](#)
38. Hu, M.L.; Li, Y.Q.; Bai, M.; Wang, Y.L.; Wu, H. Variations in volatile oil yields and compositions of *Magnolia zenii* Cheng flower buds at different growth stages. *Trees* **2015**, *29*, 1649–1660. [\[CrossRef\]](#)
39. Fanourakis, D.; Papadopoulou, E.; Valla, A.; Tzanakakis, V.A.; Nektarios, P.A. Partitioning of transpiration to cut flower organs and its mediating role on vase life response to dry handling: A case study in chrysanthemum. *Postharvest Biol. Technol.* **2021**, *181*, 111636. [\[CrossRef\]](#)
40. Dobson, H.E.M.; Danielson, E.M.; Wesep, I.D.V. Pollen odor chemicals as modulators of bumble bee foraging on *Rosa rugosa* Thunb. (Rosaceae). *Plant Species Biol.* **1999**, *14*, 153–166. [\[CrossRef\]](#)
41. Howell, A.D.; Alarcón, R. Osmia bees (*Hymenoptera: Megachilidae*) can detect nectar-rewarding flowers using olfactory cues. *Anim. Behav.* **2007**, *74*, 199–205. [\[CrossRef\]](#)
42. Raguso, R.A. Why are some floral nectars scented? *Ecology* **2004**, *85*, 1486–1494. [\[CrossRef\]](#)

**Disclaimer/Publisher’s Note:** The statements, opinions and data contained in all publications are solely those of the individual author(s) and contributor(s) and not of MDPI and/or the editor(s). MDPI and/or the editor(s) disclaim responsibility for any injury to people or property resulting from any ideas, methods, instructions or products referred to in the content.